The Distribution of Tropospheric Planetary Radiation in the Southern Hemisphere

FRANK HAURWITZ

The Rand Corporation, Santa Monica, Calif. 90406

WILLIAM R. KUHN

Dept. of Atmospheric & Oceanic Science, University of Michigan, Ann Arbor 48105

(Manuscript received 20 August 1973, in revised form 6 February 1974)

ABSTRACT

The planetary radiation for the Southern Hemisphere troposphere has been calculated from climatological data for January and July. Zonally averaged profiles of cooling/heating rates are presented. In addition, calculations have been made for selected latitudes and longitudes to illustrate the variation from the mean zonal rates. The outgoing planetary radiation and the zonally averaged net flux divergence are also discussed.

The heating/cooling rate calculations show that maximum cooling occurs in the mid-troposphere and is larger over the oceans than the continents, with longitudinal variations reaching 1C day^{-1}. Results are similar to those of Katayama for the Northern Hemisphere with the exception that we find significant heating at the base of the cirrus clouds.

The hemispheric distribution of outgoing flux agrees qualitatively with that derived from satellite measurements. The annual longitudinally averaged results agree closely with those of Sasamori *et al.* except in the vicinity of the polar front where our outgoing fluxes are about 25 ly day^{-1} smaller while in the polar latitudes our results are larger by a comparable amount. Many of the variations are directly attributable to cloud cover and the need for additional cloud data is emphasized.

1. Introduction

Relatively few studies have been made of the planetary radiation of the Southern Hemisphere, and while there is a need for improvement of the climatological data, especially cloud data, one should be able to determine the mean zonally averaged climatological cooling rates. In addition, an estimate of the longitudinal variations should be possible.

Previous theoretical studies have been carried out by Sasamori *et al.* (1971), Dopplick (1972) and Gabites (1960). Sasamori *et al.* calculated both the radiative fluxes at the boundaries of the atmosphere and the net cooling rates for the entire atmospheric column as functions of latitude. They found that the planetary flux at the top of the atmosphere has maxima at approximately 25S (518 ly day^{-1}) in the summer (January) and 15S (525 ly day^{-1}) in the winter (July). Minimum fluxes of $\sim$300 ly day^{-1} appear near the pole for both seasons. Poleward of 20S the summer values are larger than the winter values. Dopplick's study includes flux divergences for selected pressure levels to a height of about 30 km. His outward fluxes are larger at all latitudes than those of Sasamori *et al.*, with maximum values at the equator of 559 and 568 ly day^{-1} in summer and winter respectively. Maximum cooling rates occur in the mid-troposphere where, in low latitudes, the cooling reaches -2.5C day^{-1}. Cooling generally decreases toward the pole and in high latitudes it is less than 1C day^{-1} at all levels. In the region of the tropical tropopause there is a slight heating which does not exceed 0.1C day^{-1}. Gabites' study only extended from the pole to 40S, since he was primarily concerned with the energy balance of the Antarctic. His outward planetary radiation values agree with those of Sasamori *et al.* at 45S and become progressively smaller toward the pole where the annual average difference is about 25 ly day^{-1}.

The above studies considered no longitudinal variations, i.e., atmospheric parameters were zonally averaged. The only radiative study which included such variations was that carried out by Katayama (1966, 1967a,b) for the Northern Hemisphere.

The present study includes the results of a series of tropospheric infrared flux calculations for the Southern Hemisphere for January and July climatological conditions. Calculations were made for every 40° of longitude as well as for 20E and 60W. The meridional grid spacing was 10° and the vertical spacing 65 mb extending from the surface to 137 mb.

2. Methodology and data

Atmospheric fluxes were determined from numerical solutions of the integral form of the transfer equation:

$$\left.\begin{aligned} F\uparrow(u_0)&=\sum_i \pi\left[\tau_f{}^i(u_0)\int_{\delta i} B_\omega{}^i(0)d\omega \right.\\ &\qquad \left.+\int_{\delta i} B_\omega{}^i(u)d\omega\int_0^{u_0} d\tau_f{}^i(u_0-u)\right]\\ F\downarrow(u_0)&=\sum_i \pi\int_{\delta i} B_\omega{}^i(u)d\omega\int_{u_\infty}^{u_0} d\tau_f{}^i(u-u_0) \end{aligned}\right\}, \quad (1)$$

where $F\uparrow$ and $F\downarrow$ refer to the upward and downward fluxes respectively at the level corresponding to a mass path u_0, referenced from the surface; $\tau_f{}^i$ is the mean flux transmissivity (diffusivity factor of 1.667) for a spectral interval of width δ_i where the index i runs over the 18 spectral intervals used in the calculations; and $B_\omega(0)$ and $B_\omega(u)$ are the Planck functions for the surface and level u respectively. The integration over wavenumber ω for each of the i spectral intervals was carried out using a six-point Gaussian quadrature while the integration over the transmissivity was evaluated as the sum of finite differences.

The atmosphere from the surface to 100 mb was divided into layers approximately 65 mb thick, a convenient thickness for the modeling of the clouds. The fluxes were calculated at the center of each layer rather than at the boundaries of the layer since this procedure produces a smoother vertical profile of the flux divergence.

The heating/cooling rate $\Delta T/\Delta t$ was then calculated from

$$\frac{\Delta T}{\Delta t}=\frac{g\Delta F}{c_p\Delta p}, \quad (2)$$

TABLE 1. Intervals used for the individual treatment of water vapor, carbon dioxide and ozone, and for the entire infrared spectrum. Intervals are in terms of wavenumber (cm^{-1}).

Water vapor	Carbon dioxide	Ozone	Infrared
0–220			0–220
220–440			220–440
440–800			440–500
	500–555		500–555
	555–610		555–610
	610–668		610–668
	668–720		668–720
	720–775		720–775
	775–862		775–800
800–1250			800–862
			862–971
		971–1109	971–1109
			1109–1250
1250–1420			1250–1420
1420–1590			1420–1590
1590–1845			1590–1845
1845–2100			1845–2100
2100–2450			2100–2450

where $\Delta F/\Delta p$ is the vertical radiative flux divergence, g the acceleration due to gravity, and c_p the specific heat of air at constant pressure.

In order to take into account the effect of cloudiness on the flux calculations, clouds were assumed to be randomly distributed except where they occurred at the same height. Thus, the fractional amount of sky covered by overlapping clouds equals the product of the fractional covers of the individual types. As an example consider an atmosphere having clouds at two different levels, the upper deck having a fractional cover C_1 and the lower deck a fractional cover C_2. The downward flux below the lower cloud layer will consist of a clear sky contribution, and contributions from each of the cloud layers. If f_1, f_2 and f_{clear} represent the downward fluxes reaching the level at which the flux is to be determined from cloud types 1 and 2 and from the clear sky, then the total downward flux at that level will be $(C_1-C_1C_2)f_1+C_2f_2+(1-C_1-C_2+C_1C_2)f_{\text{clear}}$. Clearly with five possible cloud layers, as assumed in this study, the equations are somewhat cumbersome; however, they pose no numerical difficulties.

We treated all the clouds as blackbodies (McDonald, 1960; Havard, 1960; Widger *et al.*, 1966) except for cirrus. For these clouds we assumed a transmissivity of 0.05 in the spectral regions from 0 to 500 cm^{-1} and 1250 to 2450 cm^{-1}. The remaining parts of the spectrum were assigned a transmissivity of 0.80. These values are consistent with the work of Fritz and Rao (1967) and Kuhn and Weickmann (1969) when their results are scaled to a cirrus thickness of 1.1 to 1.8 km, the range of thicknesses used in this study.

By requiring the clouds to assume fixed heights over a given season, as is done in this model, unrealistically large heating/cooling rates (over 8C day^{-1}) may be obtained. To avoid this the heating/cooling rate for any particular layer was represented by a weighted average with the adjacent layers. Physically, this is equivalent to allowing the cloud top and base to be found 25% of the time in the layers above and below, respectively, the layer which is specified. Clearly this procedure only smooths the rates and does not change the overall flux divergence.

The transmission functions were determined theoretically from band parameters for each of the 18 spectral intervals shown in Table 1 with the exception of the 9.6-μm ozone band (971–1109 cm^{-1}) for which the empirical formula of Walshaw (1957) was adopted. Otherwise the quasi-random band model (Wyatt *et al.*, 1962) was used, i.e.,

$$\tau_f{}^i(|u-u_0|)=\prod_{j=1}^{5}\left\{\frac{1}{2}\int_{-1}^{1}\exp\left[-\frac{\rho^2\xi_j}{\eta^2+\rho^2}\right]d\eta\right\}^{n_j}, \quad (3)$$

where $\rho=2\alpha_L/\delta$, $\eta=2(\omega-\omega_0)/\delta$, and

$$\xi_j=1.667S_j|u-u_0|/(\pi\alpha_L);$$

n_j and S_j are the number of lines and the mean line

strength of the jth intensity decade of the spectral interval under consideration; and ω_0 is the wavenumber at the center of that spectral interval. The pressure-broadened half-width α_L for an arbitrary pressure p and temperature T is given by

$$\alpha_L=\alpha_0 p_{CG}\sqrt{T_0}/(p_0\sqrt{T}),$$

where p_{CG} is the Curtis-Godson pressure, α_0(NTP) the mean half-width, and p_0 and T_0 the standard pressure and temperature. For the range of temperatures encountered in the troposphere the square-root temperature correction may be neglected. Where the spectral intervals for the individual gases overlapped, the resultant transmissivities were formed from the products of transmissivities of the individual gases.

The line strengths and numbers of lines for the 15-μm band of carbon dioxide were taken from Drayson (1970, private communication), and from Benedict and Calfee (1967) and Benedict and Kaplan (1964, private communication) for the water vapor lines in the spectral region from 0 to 2450 cm^{-1}. From these data, line strengths were generated for temperatures from 150 to 325K at intervals of 25K. Regression equations were then developed for the line strengths and numbers of lines as functions of temperature for each of the five intensity decades for each of the spectral intervals. The temperature over the mass path was defined as $\int T du/\int du$.

The spectral intervals were selected to bring the transmissivities, as calculated from the quasi-random band model, into good agreement with the experimental transmissivities. A more detailed comparison is given in Haurwitz (1972). The 80-μm water vapor transmissivities are in excellent agreement with the experimental results of Palmer (1960) while the 6.3-μm values generally fall within the experimental uncertainty of Burch *et al.* (1962) except at low pressures (130 mb) and mass paths (0.002 gm cm^{-2}). The differences between the theoretical results of Rodgers and Walshaw (1966) and Burch *et al.* are of the same magnitude as the differences between our values and Burch *et al.*'s. A comparison of our 15-μm CO_2 total band absorptivities with those of Burch *et al.* indicates that our results are within the estimated range of experimental error of 5%. For the 9.6-μm O_3 band Walshaw states that the overall error in his empirical formula is about 2.4%.

The atmospheric parameters required for the radiative calculations are the temperature, pressure, and concentrations of water vapor, carbon dioxide and ozone. Total cloud cover, cloud cover by type, cloud thickness and height, and cirrus transmissivity are also necessary.

Dew point and ambient air temperatures were taken from Taljaard *et al.* (1969) in which air temperatures are provided for the surface, 850, 700, 500, 300, 200 and 100 mb and dew point temperatures for the surface, 850, 700 and 500 mb. These data were fitted to polynominals in order to provide values at the reference levels selected for the model. Above 500 mb, Mastenbrook's (1968) measurements of frost point were used. The mass mixing ratio of CO_2 was assumed to be 4.56×10^{-4} gm gm^{-1}. Since few O_3 data are available for the Southern Hemisphere, we used Dopplick's (1972) meridional profiles which were seasonally transposed from the Northern Hemisphere with a correction applied to account for the hemispheric differences in the total O_3 amounts.

Clouds constitute one of the most critical and poorly dealt with aspects of the tropospheric radiative transfer problem. Much of the difficulty is simply due to a lack of data. For this study we used the total cloud cover given by van Loon (1972) and presented in Fig. 1. Note that the cloud cover is generally smaller over the continental areas. In both seasons the cover reaches a maximum value of around 80% in the region of the polar front.

The clouds were divided into five types: Ci (cirrus, cirrostratus, cirrocumulus); As (altocumulus, altostratus); St (stratus, stratocumulus), Cb (cumulonimbus); and low (cumulus, nimbostratus). Over the oceans McDonald's (1938) values for the frequencies of occurrence of each type were used directly except for the Pacific where the cover was measured at night. There the Ci amounts were increased by 20–25% to allow for the difficulty in observation.

McDonald's (1938) values generally do not extend poleward of 50S nor is there much else directly available for this region. Thus, we assumed that the Southern Hemisphere in these latitudes has a cloud cover which approximates that of the Northern Hemisphere for similar seasons and regions. Sherr *et al.* (1968) examined this assumption and suggested that the globe can be divided into 29 homogeneous cloud climatic regions and that some of these regions can be paired as seasonal reversals. Comparing the data of Sherr *et al.* with those of McDonald suggests that this approach is justified. In the absence of data for the Antarctic, the zonally averaged frequencies of Telegadas and London (1954) for the Arctic were used.

The cloud cover over Australia was characterized by extrapolating McDonald's data inland, keeping in mind that much of that continent has a desert climate. This process was facilitated by using the climatological information of van Loon, Sherr *et al.*, Sellers (1958), Haurwitz and Austin (1944) and Shaw (1936). Cloud covers over South America and Africa are more uncertain. Frequencies of occurrence for Cb were estimated from the work of Haurwitz and Austin, and Shaw's precipitation maps were used to determine nimbostratus coverage. For the remaining cloud types we assumed that the frequencies decrease inland, and extrapolated McDonald's oceanic values onto the land areas. In order to improve this approach, Köppen's scheme of climatic classification was used to identify land regions which possess climatic characteristics

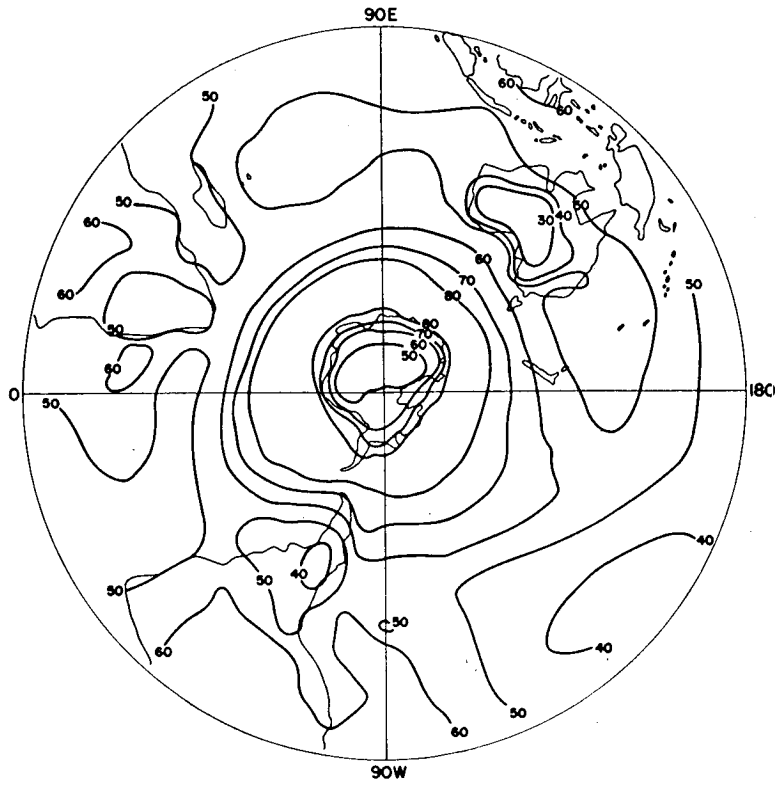

a. January

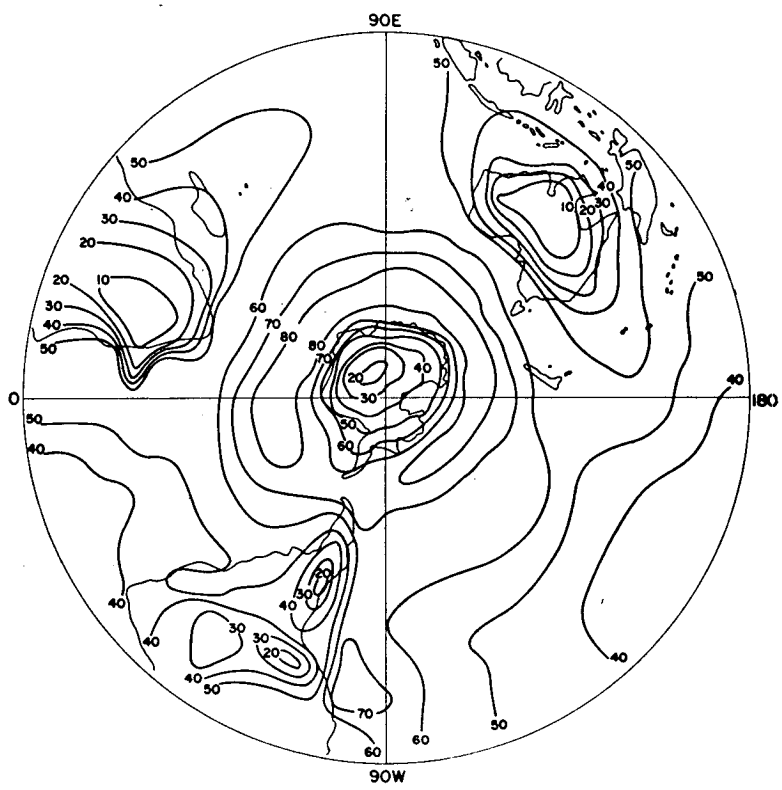

b. July

FIG. 1. Distribution of total cloud cover (percent of sky covered) over the Southern Hemisphere in January, a., and July, b.

similar to ocean regions for which cloud frequencies are known. Seasonal variations in frequency of occurrence for different cloud types over Africa and South America were assumed to parallel the variation in total cloud cover.

In order to correct for the underestimation of As and Ci we utilized a procedure suggested by Telegades and London in which the ratio of the observed cloud cover of As or Ci to the total observed sky is equal to the same ratio for the entire sky.

The most extensive surveys of cloud heights are those of Telegadas and London (1954) and Seide (1954) and their longitudinally averaged Northern Hemisphere values were used in this study. It should be noted that these heights are based primarily on observations made over land. Since it is reasonable to assume that the latitudinal variations which occur in observations made exclusively over either land or water are similar in profile and differ primarily by a scaling factor, the use of these heights for the Southern Hemisphere, which is covered primarily by ocean surface, should mainly introduce errors in the absolute magnitudes of the heights and not in their relative latitudinal variations.

One might question why the scheme developed by Katayama (1966) for expressing cloud heights in terms of the surface pressure and the pressure at the cirrus base was not used in this study. We found significant variations between heights given by Telegadas and London and those predicted by Katayama's formulation when the data of Telegadas and London were used; e.g., there are differences in height as large as 3 km for altostratus clouds.

The bases of the St, Cb, and low clouds were forced to lie at the same level, their common base being formed from the weighted mean of their individual bases. The tops of low clouds were similarly calculated from the cumulus and nimbostratus tops. In addition, the cloud heights were further adjusted by requiring their tops and bases to coincide with the nearest interfaces between atmospheric layers, an approximation which is necessary to make the heating/cooling rate calculations tractable.

Tops and bases are presented by Telegadas and London for all but St and Ci for which only bases are given. Thicknesses equal to that of one atmospheric layer (65 mb) were assumed for these two cloud types. This implies that St thicknesses range from about 0.5–0.75 km, while Ci thicknesses range from about 1.1–1.8 km. These thicknesses agree well with those reported by Tverskoi (1965). The distribution of cloud layers is shown in Fig. 2.

3. Results

a. Outgoing planetary radiation

Zonal averages of the annual outgoing planetary radiation at the top of the atmosphere from this as well as from other investigations are shown in Fig. 3. Since our calculations only extended to 137.5 mb and therefore did not include the contribution to the outward flux from the stratosphere, we have added the outgoing stratospheric contribution as calculated by Longon (1957) to our values.

The slight maximum observed around 15S results from the smaller amounts of cloudiness at those latitudes, especially in July. At higher latitudes, the flux decreases primarily because of the poleward decrease of temperature and increase in total cloud cover.

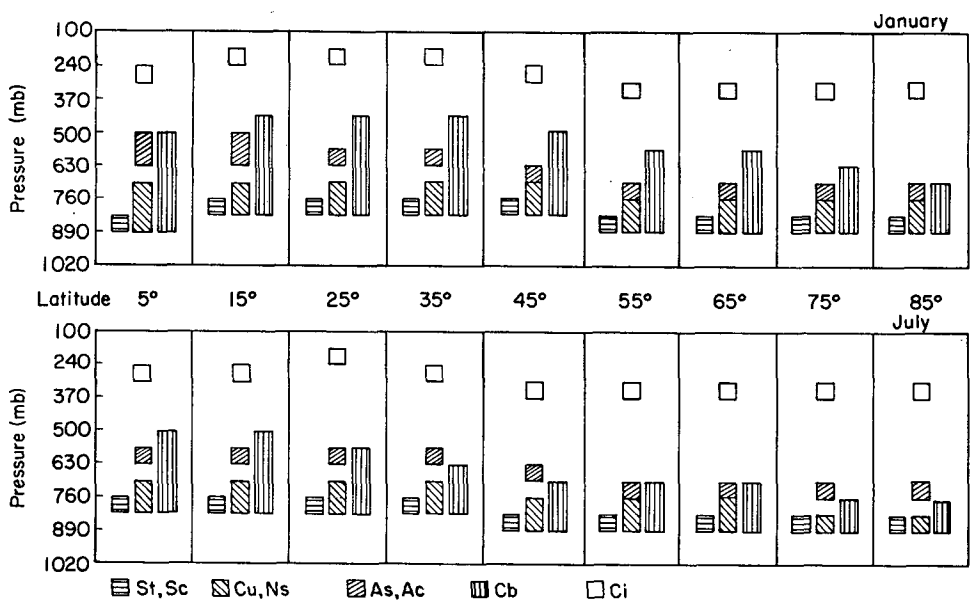

FIG. 2. Latitudinal distributions of cloud heights (this figure should not be viewed as indicating the degree of cloud overlap).

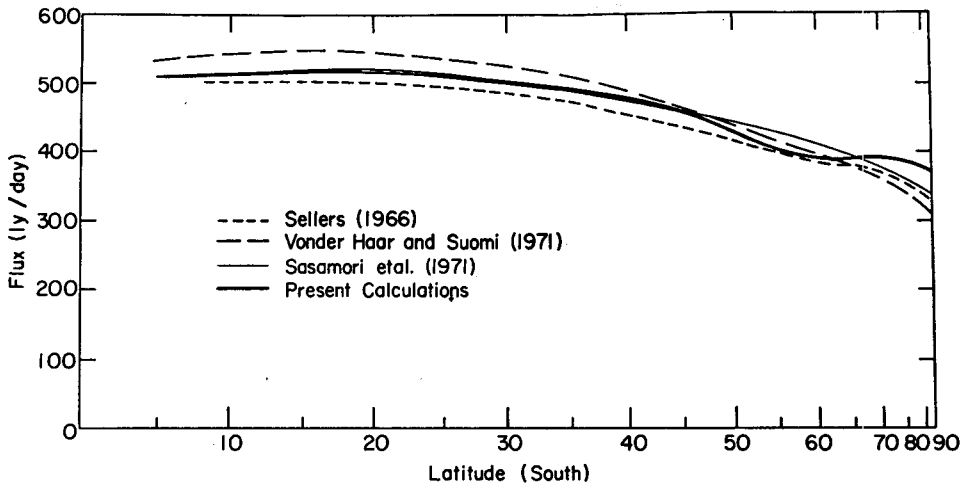

FIG. 3. Comparison of calculated and observed annual mean meridional distribution of outgoing infrared flux at the top of the atmosphere.

The rapid decrease at the polar front from about 50 to 65S shown by the present calculations and to a lesser extent by Sellers (1966) coincides with the zone of maximum cloud cover. In polar latitudes, the slight increase in flux is due to both the smaller cloud cover and the January values of temperature which increase poleward in the low stratosphere. Seasonally, the outgoing flux is larger in July from the equator to 25S and smaller at higher latitudes. In the equatorial and tropical regions the Ci cover, which is greater in January, decreases the outgoing radiation while in middle and high latitudes the warmer summer tropospheric temperatures of January are responsible for the larger fluxes.

The present calculations and those of Sasamori *et al.* (1971) are in excellent agreement up to about 45S. Between 45 and 65S the values of Sasamori *et al.* are somewhat larger which would appear to result from the smaller cloud covers used in their study. In polar latitudes our larger flux values are probably due to the use of a smaller As cover. For instance, at 75S our cover is $\sim$8.5% while Sasamori *et al.*'s is $\sim$14%.

It is not presently possible to explain the discrepancies between the satellite results of Vonder Haar and Suomi (1971) and our theoretical values. Certainly the theoretical calculations should be improved, especially with respect to the cloud data and cirrus transmissivities. However, considerable disagreement also has arisen in the interpretations of the available satellite data itself (see, e.g., Winston, 1972, and Suomi and Vonder Haar, 1972).

Hemispheric maps of outgoing flux for January and July are presented in Fig. 4. The flux patterns are primarily a function of the spatial distributions of temperature and cloud cover. A zonal pattern is apparent from the polar regions to mid-latitudes, while in the equatorial and tropical latitudes longitudinal variations appear, and are associated with the African, South American and Australian continents. In July, the fluxes are larger over the land masses than over the adjacent oceans. This same pattern is evident in the cloud cover in Fig. 3 where the regions of smaller cloud cover are associated with regions of greater flux. The same is true in January in middle and tropical latitudes, but in the equatorial regions over Indonesia, Africa and South America, the fluxes are larger over the oceans. This occurs because of the increased summertime convective activity over land and the associated increase in cloudiness.

When the present study's mean annual outgoing hemispheric fluxes and the satellite measurements analyzed by Vonder Haar and Suomi (1971) are compared, both studies are found to have a rather regular zonal pattern from the subtropics to the pole with minimum values at the pole which differ by about 6%. Over Australia, both show local maxima of about 2.75×10^5 ergs cm^{-2} sec^{-1}. Also both distributions show a tongue of smaller fluxes extending toward the equator from about 35S, although Vonder Haar and Suomi find this over South America while we find it just off the west coast. The largest differences between the two sets of results are over Africa where we find a local maximum in the outgoing flux while they show a minimum. However, in this region our results indicate that there is a local maximum in July and a minimum in January implying that the annual pattern is quite sensitive to seasonal values.

b. Net flux divergence for the atmospheric column

The mean meridional net infrared flux divergences for January and July are shown in Fig. 5. The general decrease in the divergence with increasing latitude results from a corresponding poleward decrease in the water vapor. In addition to water vapor, cloudiness (especially Ci) also plays an important role since the

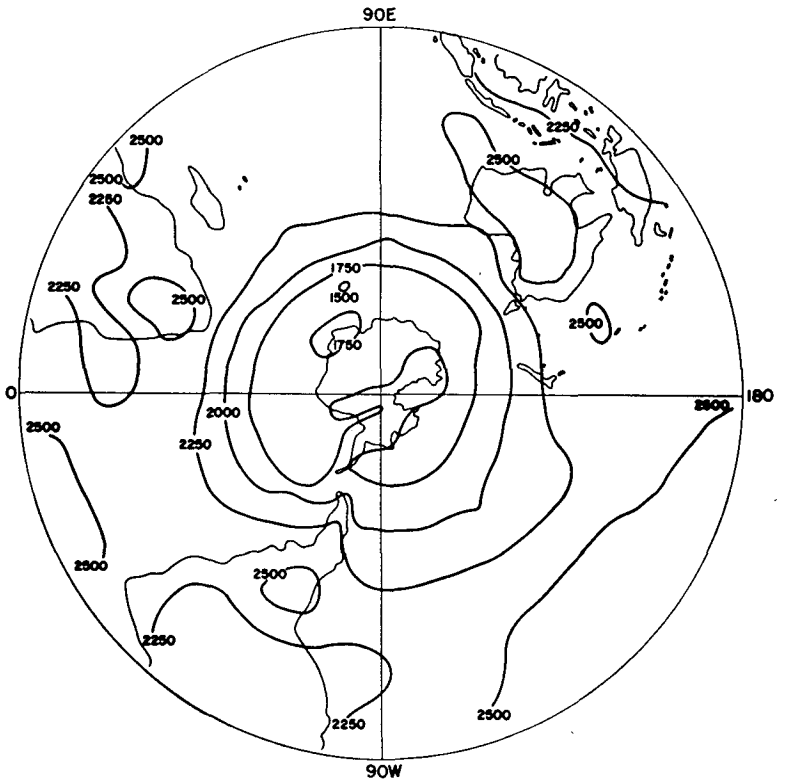

a. January

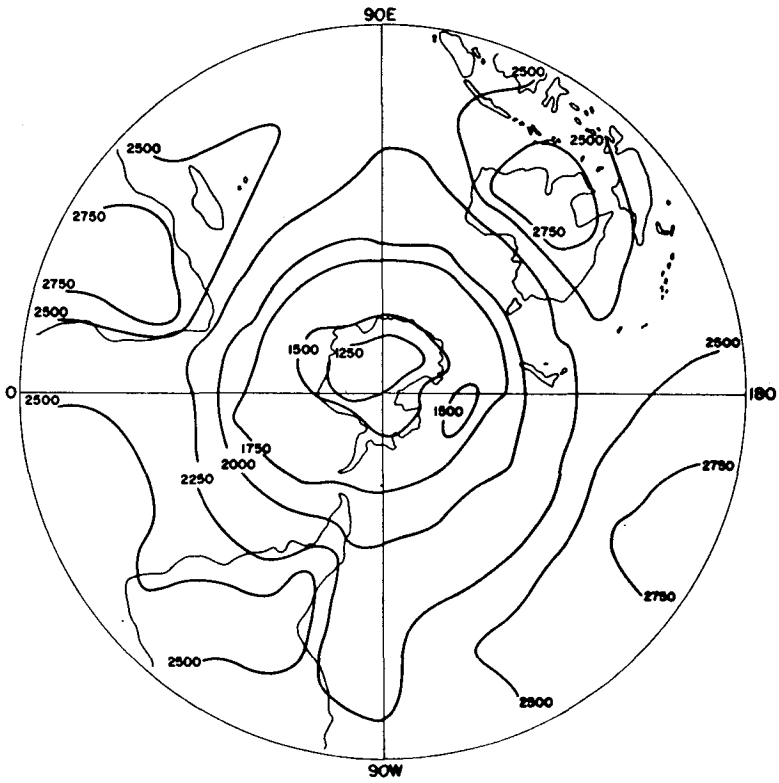

b. July

FIG. 4. Distribution of the outgoing infrared flux (units, 10^2 ergs cm^{-2} sec^{-1}) at the 137.5-mb level over the Southern Hemisphere in January, a., and July, b.

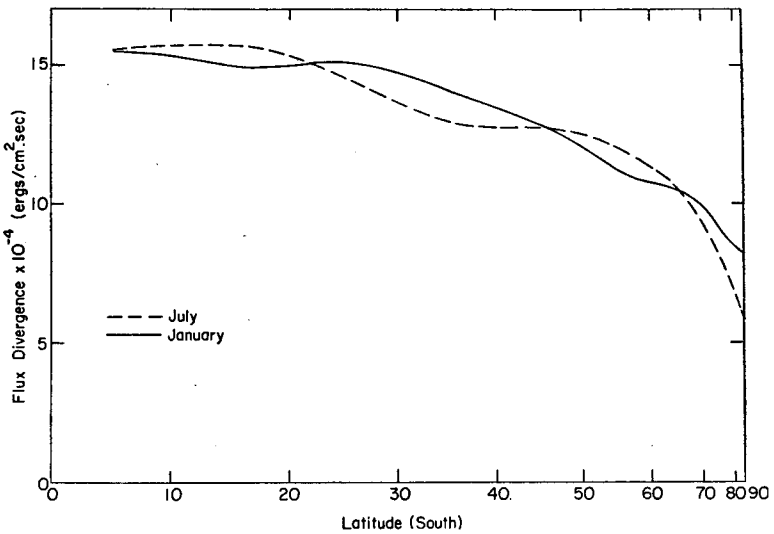

FIG. 5. Zonally averaged meridional distributions of the net infrared flux divergence (ground to 137.5 mb).

primary contribution to the net flux divergence is found at the top of the atmospheric column rather than at the ground where the net flux is small. In the tropics and mid-latitudes Ci clouds occur at lower elevations and their coverage is larger in January than July; thus, the July flux divergences are greater. In the subtropics and

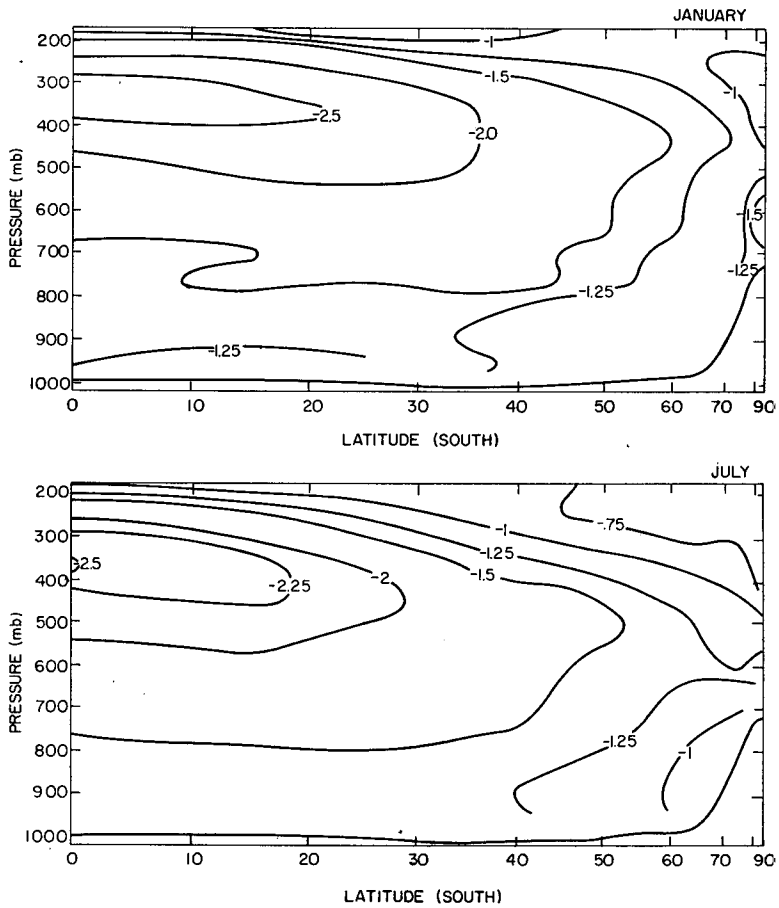

FIG. 6. Clear sky infrared cooling rates (°C day^{-1}) calculated from zonally averaged atmospheric parameters for January and July.

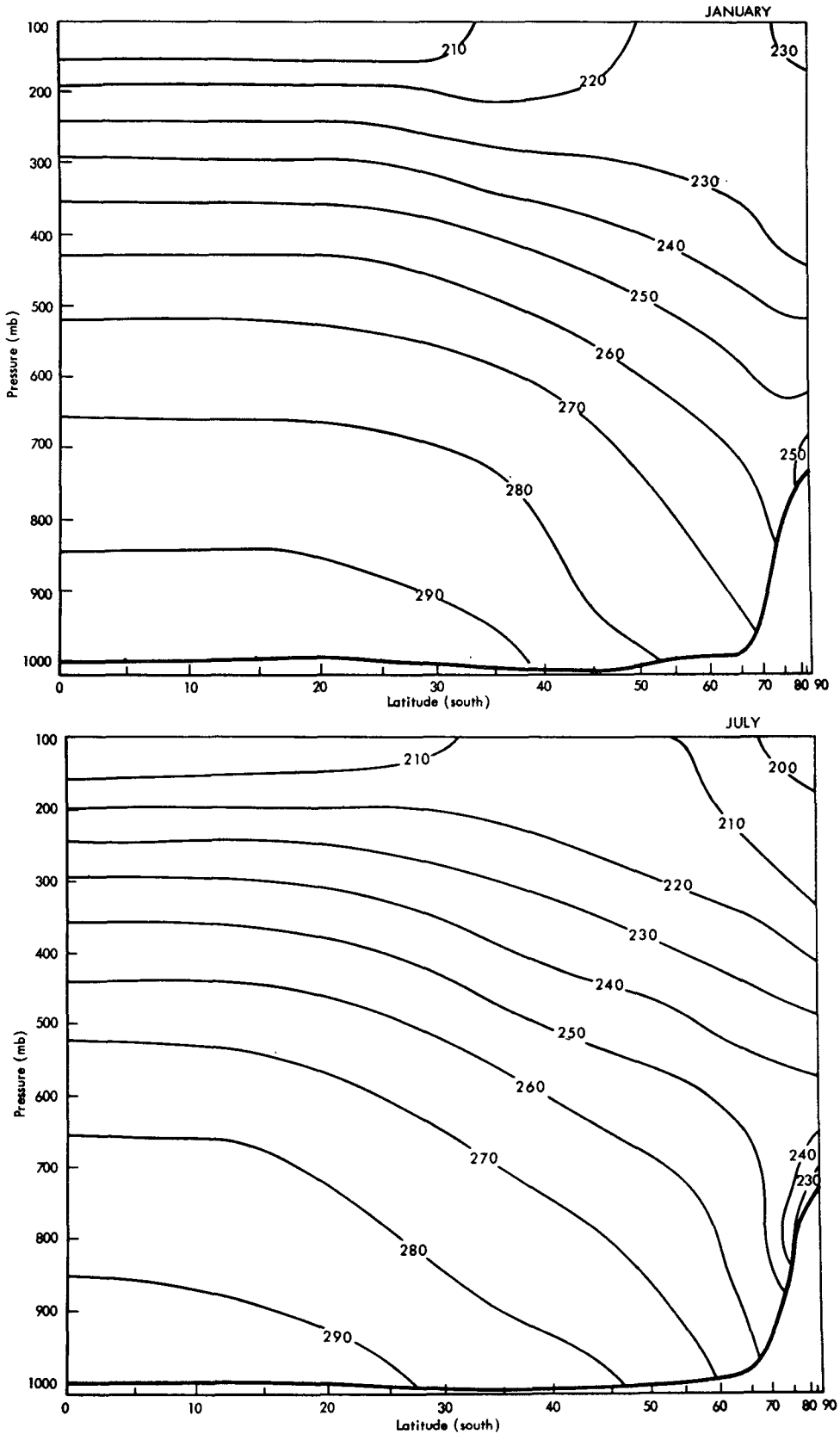

FIG. 7. Zonally averaged temperature distribution for January and July.

the polar latitudes the Ci cover is not as important since it shows little seasonal variation in the subtropics and is quite small in the polar regions. Thus, the water vapor which is greater in January controls the seasonal fluctuations at these latitudes and the flux divergence is greater in January. The relatively rapid decrease of

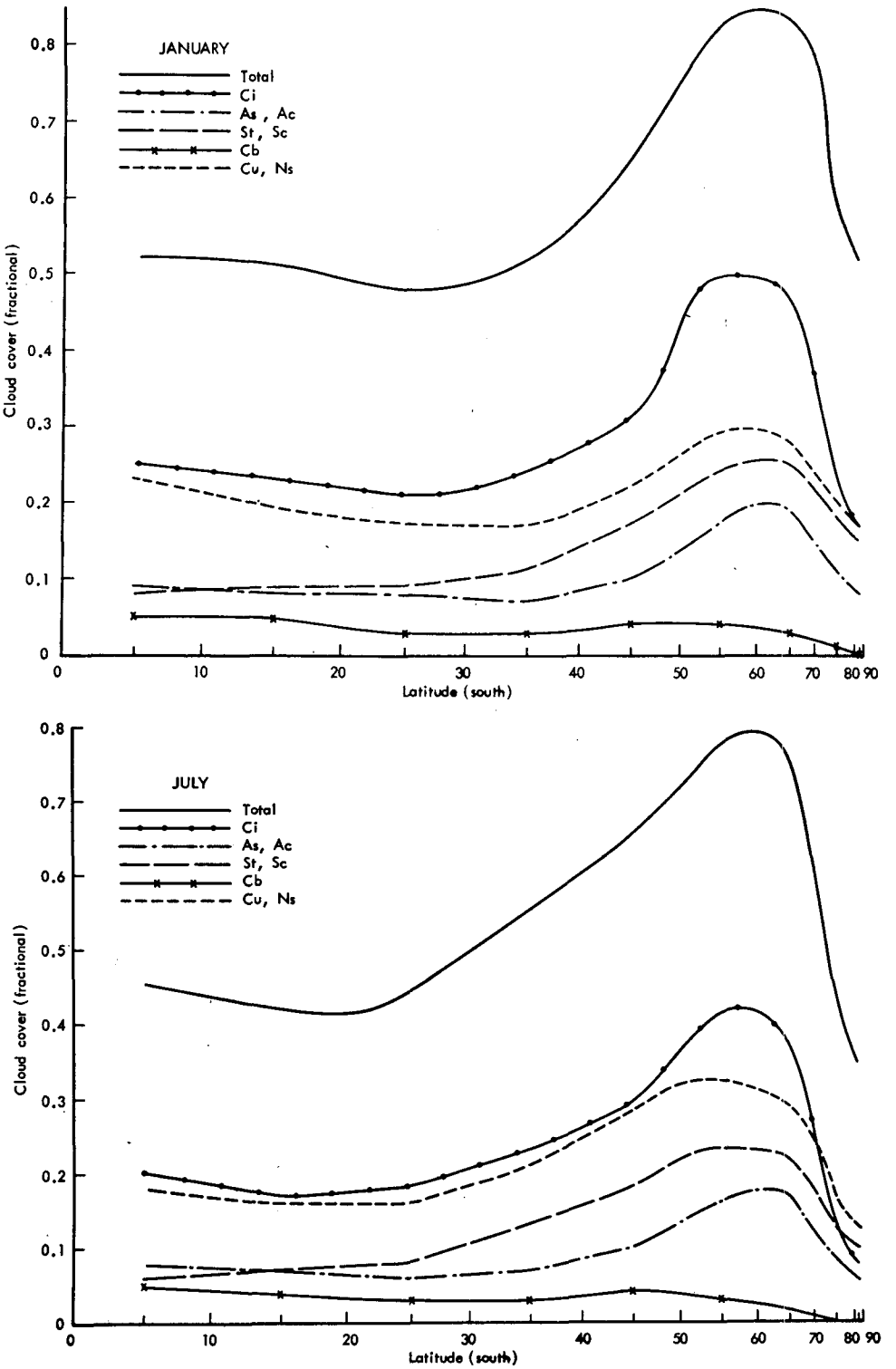

FIG. 8. Zonally averaged cloud cover for January and July.

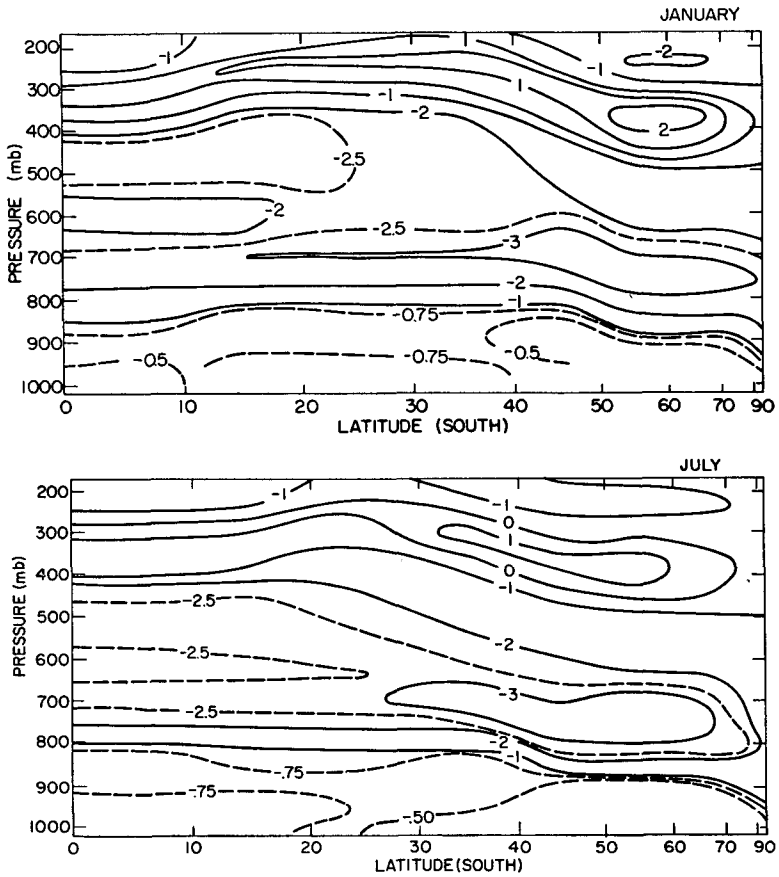

FIG. 9. Zonally averaged infrared heating and cooling rates (°C day^{-1}) for January and July with clouds present.

the divergence at high latitudes in July appears to be caused by the sharp decrease in temperature with latitude found aloft in polar latitudes.

The annual net infrared flux divergences of the present study are smaller than those of Sasamori *et al.* (1971) except near the pole where the two studies give nearly the same results. Both at the surface and top of the atmosphere their outgoing flux values are larger. The difference is thought to be due to the use of somewhat different cloud covers and heights.

c. Zonally averaged infrared heating/cooling rates

Clear sky cooling rates are shown in Fig. 6 and are presented so as to distinguish the influence of water vapor and temperature (Fig. 7) from that of clouds (Fig. 8). Cooling rates generally increase from July to January and from pole to equator. Only near the surface equatorward of 45S is the cooling greater in July. The elevation of maximum cooling (-2.5C day^{-1}) decreases from about 300 to 400 mb at the equator to greater than 600 mb at the pole. These clear sky results follow closely the temperature distribution (Fig. 7), e.g., the minimum in the high polar latitudes occurs near the polar inversion.

Fig. 9 presents the zonally averaged infrared heating/cooling rates when clouds are included in the model. The rather simple clear sky patterns have now been replaced by more complex patterns of strong cooling directly above the clouds (see Figs. 2 and 8) and weak cooling beneath, except for Ci where moderate heating occurs. This warming is strongest over the polar front where the Ci cover is greatest. Also note that the region of maximum cooling is no longer located in the equatorial region but is found in the mid-latitudes at a somewhat lower elevation.

In the tropics two layers of relatively strong cooling at about 500 and 700 mb are separated by a layer of somewhat smaller cooling rates. The strong cooling at 500 mb is the result of the increased radiative cooling near the tops of the As clouds while at 700 mb it is the result of the cooling near the tops of the low and St clouds (see Fig. 2). The decrease in cooling near 600 mb is the consequence of the increased downward flux from the bases of the As clouds. In middle and high latitudes there is a single somewhat stronger layer of maximum cooling around 750 mb which occurs because the As and lower clouds are contiguous, or nearly so. Further toward the pole the height of the cloud tops

decreases; consequently, the layer of maximum cooling is also found at lower levels. In the layers near the earth's surface the level of minimum cooling closely follows the shifting height of the common base of the lowest three cloud types.

Dopplick (1972) has also calculated zonally averaged cooling rate cross sections for the Southern Hemisphere. In his work the zone of maximum cooling in the tropics above the lower and middle clouds is evident and of the same magnitude as we found. However, poleward of 30S his cooling rates decrease and his level of maximum cooling increases with increasing latitude while our results indicate just the reverse. In the upper troposphere, Dopplick's study shows no heating, and his tropical values near the surface are over twice as large as ours.

Dopplick's cloud parameters were derived from satellite photographs taken in 1968 and supplemented by Gabites (1960) high-latitude cloud amounts and London's (1957) cloud amounts by type and cloud heights and thicknesses. Dopplick states that the percentage of high clouds is probably underestimated, which could explain the lack of heating near the tropopause. While there are differences in the number of cloud layers (Dopplick used three and we used five), as well as heights and thicknesses, we suspect most of the discrepancy occurs because Dopplick's cloud cover is primarily for a one-year period while ours is climatological.

d. Global distribution of infrared heating/cooling rates

Vertical profiles of the heating/cooling rates for January and July were calculated at 10° intervals from 5S to 85S for every 40° of longitude as well as for longitudes 20E and 60W. In addition, longitudinal cross sections at 5, 25, 45 and 75S were constructed.

The longitudinal variations in the heating/cooling rates are quite evident in the upper troposphere in the region of heating located just below the Ci clouds. At the polar front where the heating is maximum rates vary from 3.7C day^{-1} at 80E in January to 1.4C day^{-1} at 60W in July. At these levels the meridional variations are as large as 5C day^{-1} (20E, January) while the longitudinal variations reach 3C day^{-1} (25S, July). In general the largest heating values are found over the oceans.

In the mid-troposphere at middle and high latitudes the longitudinal variations of the cooling rates do not exceed 0.5C day^{-1} while in lower latitudes they are approximately twice as large. The double maxima of cooling at 700 and 500 mb found in the tropical latitudes for the zonally averaged cross sections appear in most of the individual meridional cross sections also. The seasonal variations are of about the same magnitude as their longitudinal counterparts in the mid-troposphere.

In the lower troposphere neither the longitudinal nor seasonal variations of the cooling rates are very large. The longitudinal variations reach about 0.5C day^{-1} in January at 25S and in July at 5S. The seasonal differences are smaller with values of about 0.25C day^{-1} being attained in low and mid-latitudes.

These results generally agree with those presented by Katayama (1967b) in his study of the Northern Hemisphere. There, as in the present study, maximum cooling is found to occur in the mid-troposphere and to be greater over the oceans while in the lower troposphere the cooling is greater over the continents. Our results are a few tenths of a degree per day larger than those of Katayama in the mid-troposphere and smaller by a comparable amount in the low troposphere.

The most substantial difference between the two studies occurs in the upper troposphere where Katayama (1967b) only finds a decreased cooling while we find that heating actually occurs. A number of factors may contribute to this difference. Certainly the hemispheric differences in the temperature, water vapor concentration, and Ci cover play important roles. In addition, contrary to the procedure employed in this study, Katayama (1966) assumed that there was no overlapping between the different cloud layers. In considering this assumption he showed that when overlapping is assumed there will be greater cooling at the tops and heating at the bases of the clouds as we have found. Finally, it is possible that although similar smoothing procedures were employed for the heating/cooling rates some differences will arise because we smoothed over a vertical interval of 185 mb while Katayama used 300 mb.

4. Conclusions

Tropospheric planetary heating/cooling rates have been calculated for the Southern Hemisphere for January and July. Variations in the rates are largest in the upper troposphere, with longitudinal variations reaching 3C day^{-1}. In general, heating, or at least only slight cooling, dominates this region. In the middle and low troposphere, longitudinal variations are generally less than 1C day^{-1} and 0.5C day^{-1}, respectively.

The global variations in the heating/cooling rates shown by this study of the Southern Hemisphere are comparable to those of Katayama (1967b) for the Northern Hemisphere except in the upper troposphere where Katayama does not find that any heating occurs. Rather poor agreement is found between our zonally averaged heating/cooling rate profiles and those of Dopplick (1972) where there are not only quantitative but also qualitative differences, especially at high latitudes.

The present zonally averaged outgoing radiation values agree well with those of Sasamori *et al.* (1971) from the equator to the mid-latitudes. However, in the

vicinity of the polar front, our values are somewhat smaller while further south they are larger.

It is obvious that both the magnitudes and spatial distributions of the heating/cooling rates are critically dependent on cloud cover and attempts presently being made to deduce cloud heights and amounts from satellite observations should provide much of the needed data.

Acknowledgments. Support for this work was provided by the National Science Foundation under Grant GA-10884. Acknowledgment is made to the National Center for Atmospheric Research, which is sponsored by the National Science Foundation, for computer time used in this research.

REFERENCES

Benedict, W. S., and R. F. Calfee, 1967: Line parameters for the 1.9 and 6.3 micron water vapor bands. ESSA Professional Paper 2.

Burch, D. E., D. A. Gryvnak and D. Williams, 1962: Infrared absorption by carbon dioxide, water vapor, and minor atmospheric constituents. Research Report, Contract AF19(604)-2633, Ohio State University, 316 pp.

Clodman, J., 1957: Some statistical aspects of cirrus cloud. *Mon. Wea. Rev.*, **85**, 37–41.

Dopplick, T. G., 1972: Radiative heating of the global atmosphere. *J. Atmos. Sci.*, **29**, 1278–1294.

Fritz, S., and P. K. Rao, 1967: On the infrared transmission through cirrus clouds and the estimation of relative humidity from satellites. *J. Appl. Meteor.*, **6**, 1088–1096.

Gabites, J. F., 1960: The heat balance of the Antarctic. *Antarctic Meteorology*, London, Pergamon Press, 370–377.

Haurwitz, F. D., 1972: The distribution of tropospheric infrared radiative fluxes and associated heating and cooling rates in the Southern Hemisphere. Tech. Rept., High Altitude Engineering Laboratory, University of Michigan, Ann Arbor, 168 pp.

Haurwitz, B., and J. M. Austin, 1944: *Climatology.* New York, Mc-Graw Hill, 410 pp.

Havard, J. B., 1960: On the radiational characteristics of water clouds at infrared wavelengths. Ph.D. thesis, University of Washington, Seattle.

Katayama, A., 1966: On the radiation budget of the troposphere over the Northern Hemisphere (I). *J. Meteor. Soc. Japan*, Ser. 2, **44**, 381–401.

——, 1967a: On the radiation budget of the troposphere over the Northern Hemisphere (II). *J. Meteor. Soc. Japan*, Ser. 2, **45**, 1–25.

——, 1967b: On the radiation budget of the troposphere over the Northern Hemisphere (III). *J. Meteor. Soc. Japan*, Ser. 2, **45**, 26–38.

Kuhn, P. M., and H. K. Weickmann, 1969: High-altitude radiometric measurements of cirrus. *J. Appl. Meteor.*, **8**, 147–154.

London, J., 1957: A study of the atmospheric heat balance. Final Report, Contract AF19(122)-165, College of Engineering, New York University, 99 pp.

Mastenbrook, H. J., 1968: Water vapor distribution in the stratosphere and high troposphere. *J. Atmos. Sci.*, **25**, 299–311.

McDonald, J. E., 1960: Absorption of atmospheric radiation by water films and water clouds. *J. Meteor.*, **17**, 232–238.

McDonald, W. F., 1938: *Atlas of Climatic Charts of the Oceans.* U. S. Weather Bureau, No. 1247, Washington, D. C., Gov't. Printing Office.

Palmer, C. H., Jr., 1960: Experimental transmission functions for the pure rotation band of water vapor. *J. Opt. Soc. Amer.*, **50**, 1232–1242.

Rodgers, C. D., and C. D. Walshaw, 1966: The computation of infrared cooling rate in planetary atmospheres. *Quart. J. Roy. Meteor. Soc.*, **92**, 67–92.

Sasamori, T., J. London and D. V. Hoyt, 1971: Radiation budget of the Southern Hemisphere. Ms. No. 71-100, National Center for Atmospheric Research, 38 pp.

Seide, R. N., 1954: The distribution of cloudiness by type and height in the Northern Hemisphere for the spring and fall. M. S. thesis, New York University, 34 pp.

Sellers, W. D., 1958: The annual and diurnal variations of cloud amounts and cloud types at six Arizona cities. Sci. Rept. No. 8, Institute of Atmospheric Physics, University of Arizona, 104 pp.

——, 1966: *Physical Climatology.* The University of Chicago Press, 272 pp.

Shaw, N., 1936: *Manual of Meteorology*, Vol. 2: *Comparative Meteorology.* London, Cambridge University Press, 472 pp.

Sherr, P., A. H. Glaser, J. C. Barnes and J. H. Willand, 1968: World-wide cloud cover distributions for use in computer simulations. Final Report, Contract NAS 8-21040, Allied Research Associates, Inc., 140 pp.

Suomi, V. E., and T. H. Vonder Haar, 1972: Reply (to Winston). *J. Atmos. Sci.*, **29**, 602–607.

Taljaard, J. J., H. van Loon, H. L. Crutcher and R. L. Jenne, 1969: *Climate of the Upper Air, Part 1: Southern Hemisphere*, Vol. 1. NAVAIR 50-1C-55, U. S. Navy.

Telegadas, K., and J. London, 1954: A physical model of the Northern Hemisphere troposphere for winter and summer. Sci. Rept. No. 1, Contract AF19(122)-165, College of Engineering, New York University, 55 pp.

Tverskoi, P. N., 1965: *Physics of the Atmosphere.* Israel Program for Scientific Translations, NASA TTF-288.

van Loon, H., 1972: Cloudiness and precipitation in the Southern Hemisphere, *Meteor. Monogr.*, **13**, No. 35, 101–138.

Vonder Haar, T. H., and V. E. Suomi, 1971: Measurements of the earth's radiation budget from satellites during a five-year period: Part I. Extended time and space means. *J. Atmos. Sci.*, **28**, 305–314.

Walshaw, C. D., 1957: Integrated absorption by the 9.6μ band of ozone. *Quart. J. Roy. Meteor. Soc.*, **83**, 315–321.

Widger, W. K., Jr., J. C. Barnes, E. S. Merritt and R. B. Smith, 1966: Meteorological interpretations of nimbus high resolution infrared (HRIR) data. NASA Contractor Report CR-352, 150 pp.

Winston, J. S., 1972: Comments on "Measurements of the earth's radiation budget from satellites during a five-year period: Part I. Extended time and space means". *J. Atmos. Sci.*, **29**, 598–601.

Wyatt, P. J., V. R. Stull and G. N. Plass, 1962: Quasi-random model of band absorption. *J. Opt. Soc. Amer.*, **52**, 1209–1217.